Calculation of the strength of multilayer floor slabs supported on three sides

Oleg Korol, *Rima* Petrosyan[1,*], and *Pavel* Truntov

Moscow State University of Civil Engineering, 26, Yaroslavskoye shosse, Moscow, 129337, Russia

Abstract. The article considers the calculation of the ultimate rupture load of multilayer floor slabs supported on three sides (two short and one long). The calculation is carried out taking into account three fracture schemes: the first scheme consists of three main destructive cracks that converge at one point, forming an "envelope"; the second scheme consists of two main inclined cracks passing from the corners towards the non-supported side and not converging on the plate field; the third scheme consists of a horizontal crack forming trapezoid in combination with angular cracks, which is the case when testing prototypes. The reduction of a three-layer section to a single-layer section is carried out according to the elasticity modules of the concretes that make up the section. The value of the rupture load is determined from the condition of equilibrium of external and internal forces. The results of the VAT analysis of multilayer reinforced concrete structures according to the proposed schemes were carried out by the authors on the basis of static tests of prototypes of flat reinforced concrete three-layer slabs. The obtained research results allow us to determine rational parameters for the design of multilayer slab structures with reinforced concrete layers of various strength.

Keywords: concrete buildings, reinforced concrete, multilayer structures, three-layer structures, stress analysis.

1 Introduction

The choice of methods for calculating multilayer reinforced concrete structures is carried out taking into account the characteristic features of the design and manufacturing technology of the structures in question.

The following factors have a significant impact on the stress-strain state of a multilayer structure: physical and mechanical properties of the materials used; geometric characteristics of the structure under consideration (thickness of layers of a multilayer structure, cross-section dimensions, length of the element); geometric and physical nonlinearity; plastic and rheological properties of the materials used, the formation of cracks in the inner layer.

As a result of static tests of three-layer load-bearing slabs of interfloorings supported on three sides (two short and one long), it was determined that the destruction of the slabs was plastic in nature and began with the formation of diagonal cracks on the ceiling surface coming from the corners of the slab, then cracks parallel to the short sides in the central part of the slab. However,

* Corresponding author: PetrosyanRS@mgsu.ru

when calculating the bearing capacity of plates supported on three sides, this angle is assumed to be 45°, which increases the value of the rupture load compared to the actual by 5.2%. Therefore, when calculating the rupture load of three-layer plates supported on three sides, it is necessary to take into account the actual value of the angle φ, which is determined depending on the bending moments and geometric dimensions of the plate. The reduction of a three-layer section to a single-layer section is carried out according to the elasticity modules of the concretes that make up the section.

To calculate the ultimate rupture load of plates, three possible fracture schemes are considered (Fig. 1): the first scheme consisting of three main destructive cracks that converge at one point, forming an "envelope"; the second scheme consisting of two main inclined cracks passing from the corners towards the non-supported side and not converging on the plate field; the third scheme consisting of a horizontal crack forming trapezoid in combination with angular cracks, which is the case when testing prototypes. In the first scheme, two options are possible with a variable-pitch reinforcement: 1) the point of convergence of cracks is located under the boundary of the pitch change, 2) the point of convergence of cracks is located above the boundary mentioned.

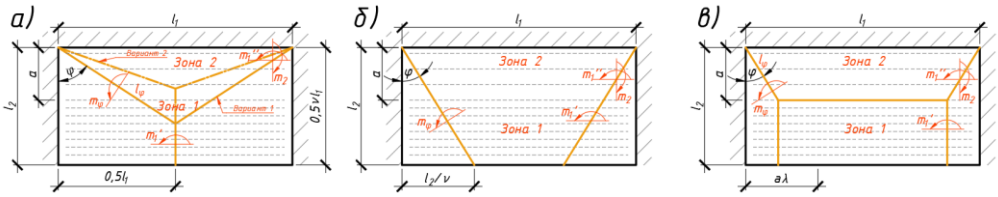

Fig. 1. Calculation schemes of plates: a – with cracks converging at one point; b – with two inclined cracks; c – with a horizontal crack. Zone 1 – the part of the plate below the boundary of the pitch change; zone 2; b – same as a, but above the boundary.

The value of the rupture load qп, corresponding to the ultimate state of strength, is determined from the condition of equilibrium of external and internal forces arising when loading plates supported on three sides, according to the design scheme corresponding to the mechanism of destruction under the action of a uniformly distributed load.

2 Materials and methods

The following characteristics of materials were adopted for the research: concrete of class B15÷B25 for the outer layers and the inner layer of lightweight concrete with low thermal conductivity properties, with compression resistance up to 7.5 MPa.

Consider the first fracture scheme. We introduce the following dependencies and designations: v=ctg φ; ɣ = l1/(2l 2); n = a/l 2; l φ = 1; l φ'=2a/(vl 1), where φ is the angle of inclination of the angular crack; l 1 and l 1 are the dimensions, respectively of the long and short sides of the plate; a – part of the short side of the plate, with a rarer rebar pitch; l φ – the length of the inclined crack; l φ' – the length of the displacement of the plate section during fracture. For option 1) a <0.5vl1, for option 2) a>0.5vl1.

The work of external forces A is the product of the force on the volume of the conditional prism formed after the destruction of the plate by the action of this force:

$$A = q_{\text{п}}\left[\left(l_2 - \frac{vl_1}{2}\right)\frac{l_1}{2} + \frac{l_1}{3}\cdot\frac{vl_1}{2}\right] = \frac{q_{\text{п}}l_1^2}{12\gamma}(3-\gamma v). \qquad (1)$$

The work of internal forces U is defined as the sum of the work of bending moments acting along the fracture line on the angles of the fracture.

We introduce the following designations: m_1'– bending moment acting on 1 lin m of plate along the span $l_1$in zone 1; m_1''– the same in zone 2; m_2– bending moment acting on 1 lin m of

plate along the spanl_2; m'_φ– bending moment acting on 1 lin m of plate along the inclined crack $l_\varphi$in zone 1; m''_φ– the same, in zone 2; θ – the angle of displacement of the angle of the fracture along the span l_1; θ_φ – the same, along the crack l_φ.

$$Here\ m'_1 = \frac{M'_1}{l_2-a};\ m''_1 = \frac{M''_1}{a};m_2 = \frac{M_2}{l_1};$$

$$m'_\varphi = m'_1 cos^2\varphi + m_2 sin^2\varphi = \frac{\nu m'_1+m_2}{\nu^2+1};$$

$$m''_\varphi = \frac{\nu m''_1+m_2}{\nu^2+1};\ \theta = \frac{4}{l_1};\ \theta_\varphi = \frac{1}{\nu l_\varphi} + \frac{\nu}{l_\varphi} = \frac{\nu^2+1}{\nu l_\varphi}.$$

Therefore:

$$U = m'_1\left(l_2 - \frac{\nu l_1}{2}\right)\theta + 2\left[m''_\varphi l''_\varphi + m'_\varphi\left(l_\varphi - l''_\varphi\right)\right]\theta_\varphi = \frac{2m'_1}{\gamma\nu}(\beta\nu + \gamma\psi') \qquad (2)$$

$$where\ \beta = 1 - \eta(1-\psi'');\ \psi' = \frac{m_2}{m'_1};\ \psi'' = \frac{m''_1}{m'_1}.$$

From the condition of equality of the work of external and internal forces (A = U) we have:

$$\frac{q_п l_1^2}{12\gamma}(3-\gamma\nu) = \frac{2m'_1}{\gamma\nu}(\beta\nu + \gamma\psi'),$$

from which:

$$q_п = \frac{24M'_1(\beta\nu+\gamma\psi')}{l_1^2(l_2-a)\nu(3-\gamma\nu)}. \qquad (3)$$

We νdetermine the parameter from the condition $min q_п \frac{\partial q_п}{\partial \nu} = 0$.After performing the necessary transformations, we obtain a quadratic equation with respect to ν: $\beta\nu^2 + 2\gamma\psi'\nu - 3\psi' = 0$, solving which we find:

$$\nu = \frac{1}{\beta}\left(\sqrt{(\gamma\psi')^2 + 3\beta\psi'} - \gamma\psi'\right). \qquad (4)$$

For the second variant of the scheme under consideration, the $a > 0{,}5\nu l_1$destructive work of internal forces is equal to:

$$U = \left[m'_1(l_2-a) + m''_1\left(a - \frac{\nu l_1}{2}\right)\right]\theta + 2m''_\varphi l_\varphi\theta_\varphi = \frac{2m'_1}{\gamma\nu}(\beta\nu + \gamma\psi').$$

The resulting value of the work of internal forces is similar to the value obtained by the formula (2) at $a < 0{,}5\nu l_1$, i.e. the action of external and internal forces does not depend on the location of the junction point of the three main destructive cracks.

For a plate reinforced with rods with a constant pitch, the work of internal forces is due to the action of bending moments along the spans l_1 and l_2 along the crack l_φ:

$$U = m_1\left(l_2 - \frac{\nu l_1}{2}\right)\theta + 2m_\varphi l_\varphi\theta_\varphi = \frac{2m'_1}{\gamma\nu}(\nu + \gamma\psi), \qquad (5)$$

$$Where\ \psi = \frac{m_2}{m_1};\ m_1 = \frac{M_1}{l_2};\ m_2 = \frac{M_2}{l_1}.$$

From the condition of equality of work of internal and external forces we have:

$$\frac{q_п l_1^2}{12\gamma}(3-\gamma\nu) = \frac{2m_1}{\gamma\nu}(\beta\nu + \gamma\psi),$$

Hence, the maximum load acting on a plate reinforced with a constant pitch is equal to:

$$q_п = \frac{24M_1(\nu+\gamma\psi)}{l_1^2 l_2\nu(3-\gamma\nu)}. \qquad (6)$$

From the condition $q_п \frac{\partial q_п}{\partial \nu} = 0$ after the transformation we get:

$$\nu = \sqrt{\gamma^2\psi^2 + 3\psi} - \gamma\psi. \qquad (7)$$

For a plate reinforced in one direction along the span l_1(i.e. with a reinforcement coefficient $\mu_2 = 0$), $m_2 = 0$. This means that $\beta = 1,\ \psi = 0$. It means the ultimate rupture load acting on the plate is equal to:

$$q_п = \frac{24M_1(\nu+\gamma\psi)}{l_1^2 l_2\nu(3-\gamma\nu)} = \frac{8M_1}{l_1^2 l_2}. \qquad (8)$$

The bending moments acting on the plate are equal to:

Along the span l_1 with a constant armature pitch:

$$M_1 = \mu_1 R_{s1} l_2 h_{01}^2 \left(1 - 0{,}5\mu_1 \frac{R_{s1}}{R_b}\right);$$

For span l_1 in zone 2:

$$M_1'' = \mu_1'' R_{s1}'' a h_{01}^2 \left(1 - 0{,}5\mu_1'' \frac{R_{s1}''}{R_b}\right);$$

Along the span l_1 in zone 1:

$$M_1' = \mu_1' R_{s1}' (l_2 - a) h_{01}^2 \left(1 - 0{,}5\mu_1' \frac{R_{s1}'}{R_b}\right);$$

Along the span l_2:

$$M_2 = \mu_2 R_{s2} l_1 h_{02}^2 \left(1 - 0{,}5\mu_2 \frac{R_{s2}}{R_b}\right),$$

Where

$$\mu_1 = \frac{A_{s1}}{l_2 h_{01}};\ \mu_1'' = \frac{A_{s1}''}{a h_{01}};\ \mu_1' = \frac{A_{s1}'}{(l_2 - a) h_{01}};\ \mu_2 = \frac{A_{s2}}{l_1 h_{02}}.$$

Consider the second fracture scheme. This scheme is only possible when $\varphi < 45°$. At the same time, the $\varphi > 45°$first fracture scheme should be taken for calculation. The designations and dependencies are the same as for the first scheme.

The work of external forces:

$$A = q_п \left[\left(l_1 - \frac{2l_2}{\nu}\right)\frac{l_2}{2} + \frac{2l_2}{3\nu} l_2\right] = \frac{q_п l_q^w}{12\gamma\nu}(3\gamma\nu - 1). \qquad (9)$$

The work of internal forces:

$$U = 2\left(m_\varphi' \frac{l_2 - a}{l_2} l_\varphi + m_\varphi' \frac{a}{l_2} l_\varphi\right)\theta_\varphi = \frac{2m_2'}{\nu}(\beta\nu^2 + \psi'). \qquad (10)$$

From the condition of equality of external and internal forces, we obtain the value of the ultimate rupture load acting on the plate:

$$q_п = \frac{24 M_1' \gamma (\beta\nu^2 + \psi')}{l_1^2 (l_2 - a)(3\gamma\nu - 1)}. \qquad (11)$$

From the condition we $min\ q_п$define the parameterν : $\frac{\partial q_п}{\partial \nu} = 0$.

After the transformation, we obtain a quadratic equation with respect to ν:

$$3\beta\gamma\nu^2 - 2\beta\nu - 3\gamma\psi' = 0,$$

Therefore

$$\nu = \frac{1}{3\gamma}\left(1 + \sqrt{1 + \frac{9\gamma^2\psi'}{\beta}}\right). \qquad (12)$$

For a plate with a constant reinforcement pitch during fraction according to the second scheme, the work of internal forces is equal to:

$$U = 2m_\varphi l_\varphi \theta_\varphi = \frac{2m_1}{\nu}(\nu^2 + \psi). \qquad (13)$$

From the condition we $A = U$get the value of the ultimate rupture load:

$$q_{\text{п}} = \frac{24M_1\gamma(\nu^2+\psi)}{l_1^2 l_2(3\gamma\nu-1)}. \qquad (14)$$

With $\frac{\partial q_{\text{п}}}{\partial \nu} = 0$:

$$3\gamma\nu^2 - 2\nu - 3\gamma\psi = 0.$$

Therefore

$$\nu = \frac{1}{3\gamma}\left(1+\sqrt{1+9\gamma^2\psi}\right). \qquad (15)$$

Consider the third plate scheme. We denote $\lambda = \frac{1}{\nu} = tan\ tan\ \varphi$, the other designations and dependencies are the same as in the first scheme.

According to the presented mechanism of destruction, the work of external forces is equal to:

$$A = q_{\text{п}}\left[\frac{l_2-a}{2}(l_1+l_1-2a\lambda)+\frac{a}{2}(l_1-2a\lambda)+\frac{2}{3}a^4\lambda\right] = \\ = \frac{q_{\text{п}}l_1^2}{12\gamma^2}[3\gamma(2-\eta)-\eta\lambda(3-2\eta)]. \qquad (16)$$

The work of internal forces is carried out under the action of bending moments m_1', m_1'', m_2 и m_φ. Here $m_\varphi = \frac{m_1''+m_2\lambda}{\lambda^2+1}$.

As a result of the destruction, the sections of the plate are displaced: along the span $l_1$at an angle $\theta = \frac{1}{a\lambda}$, along the span $l_2$at an angle $\theta_2 = \frac{1}{a}$, along the angular crack at an angle $\theta_\varphi = \frac{\lambda^2+1}{\lambda}$. Then:

$$U = 2m_1'(l_2-a)+m_2(l_1-2a\lambda)\theta_2+2m_\varphi''l_\varphi''\theta_\varphi = \frac{2m_1'}{\eta\lambda}(\gamma\lambda\psi'+\beta). \qquad (17)$$

From the condition $A = U$ we get the value of the maximum load destroying the plate:

$$q_{\text{п}} = \frac{24M_1'\gamma^2(\gamma\lambda\psi'\beta)}{l_1^2(l_2-a)\eta\lambda[3\gamma(2-\eta)-\eta\lambda(3-2\eta)]}. \qquad (18)$$

With $\frac{\partial q_{\text{п}}}{\partial \nu} = 0$:

$$\gamma\psi'\gamma^2 + 2\beta\lambda - 3\beta\gamma\frac{2-\eta}{\eta(3-\eta)} = 0. \qquad (19)$$

Denoting, $\alpha = \frac{3(2-\eta)}{\eta(3-\eta)}$,we present equation (19) in the form of:

$$\gamma\psi'\lambda^2 + 2\beta\lambda - \alpha\beta\gamma = 0.$$

Therefore:

$$\lambda = \frac{1}{\gamma\psi'}\left(\sqrt{\beta^2+\alpha\beta\gamma^2\psi'}-\beta\right). \qquad (20)$$

To determine the location of the longitudinal crack, we find the value of η.

With $\frac{\partial q_{\text{п}}}{\partial \eta} = 0$:

$$\lambda\eta = (\gamma+\lambda)\eta + \gamma = 0.$$

Therefore $\eta = \frac{\gamma}{\lambda}$.

For plates with a constant reinforcement pitch, $\psi'' = 0$,therefore, $\beta = 1$.Therefore, the ultimate rupture load is equal to:

$$q_{\text{п}} = \frac{24M_1\gamma^2(\gamma\lambda\psi + 1)}{l_1^2 l_2 \eta\lambda[3\gamma(2-\eta) - \eta\lambda(3-2\eta)]}, \quad (21)$$

$$\lambda = \frac{1}{\gamma\psi}\left(\sqrt{1+\alpha\gamma^2\psi} - 1\right). \quad (22)$$

3 Research results

The results of the VAT analysis of multilayer reinforced concrete structures according to the proposed schemes (Fig. 1) were performed by the authors on the basis of static tests of prototypes of flat reinforced concrete three-layer slabs with a thickness of h = 180 mm and dimensions in terms of 6x3 m with outer layers 45 mm thick of heavy concrete B15 and an average layer of coarse-porous expanded clay concrete B2,5. The class of reinforcement used is A400. The layers are rigidly interconnected in a single molding cycle. 3 fracture schemes were used for calculations. To conduct the study, the diameter of the reinforcement used, the reinforcement pitch, and the overall dimensions of the plate were changed. The results are shown in Table 1.

Table 1. Bearing capacity of plates with dimensions of 6x3m according to 1 fracture scheme.

Ø reinforcements	**Bending moments, kN·m**				**Calculated angle of crack inclination at variable and constant reinforcement pitch, φ**	**Maximum design loads at variable reinforcement pitch, kN/m2**	**Maximum design loads at a constant reinforcement pitch, kN/m2**	**Maximum design loads for reinforcement in one direction, kN/m2**
	M_1'	M_1''	M_1	M_2		$q_{\text{п}}^{\text{теор}}$	$q_{\text{п}}^{\text{теор}}$	$q_{\text{п}}^{\text{теор}}$
6	29.7	20.9	41.9	43.86	52°/50°	7.88	7.0	3.1
8	48.58	34.25	68.8	72.5	52°/50°	12.94	11.52	5.09
10	75.41	53.41	107.57	114.74	52°/50°	20.25	18.09	7.96
12	100.5	71.53	144.47	155.93	51°/50°	27.22	24.41	10.7
14	131.25	94.07	190.76	209.27	51°/50°	35.97	32.44	14.1
16	165.34	119.65	243.93	273.45	51°/49°	46.04	41.83	18.06

Table 2. Bearing capacity of plates with dimensions of 6x3m according to 2 fracture scheme.

Ø reinforcements	**Bending moments, kN·m**		**Calculated angle of crack inclination at variable and constant reinforcement pitch, φ**	**Maximum design loads at variable reinforcement pitch, kN/m2**	**Maximum design loads at a constant reinforcement pitch, kN/m2**
	M_1'	M_1		$q_{\text{п}}^{\text{теор}}$	$q_{\text{п}}^{\text{теор}}$
6	29,7	41,9	43°/41°	8,03	4,97

8	34,25	68,8	43°/41°	13,18	8,18
10	75,41	114,7	43°/41°	20,6	12,8
12	100,5	144,47	43°/41°	27,64	17,64
14	131,25	190,76	43°/41°	36,45	22,83
16	165,34	243,93	42°/41°	46,52	29,3

Table 3. Bearing capacity of plates with dimensions of 6x3m according to 3 fracture scheme.

Ø reinforcements	**Bending moments, kN·m**		**Calculated angle of crack inclination at variable and constant reinforcement pitch, φ**	**Maximum design loads at variable reinforcement pitch, kN/m2**	**Maximum design loads at a constant reinforcement pitch, kN/m2**
	M_1'	M_1		$q_{\text{п}}^{\text{теор}}$	$q_{\text{п}}^{\text{теор}}$
6	29,7	41,9	57°/56°	8,48	7,64
8	34,25	68,8	57°/56°	13,95	12,59
10	75,41	114,7	57°/56°	21,85	19,79
12	100,5	144,47	57°/56°	29,4	26,7
14	131,25	190,76	56°/55°	38,92	35,56
16	165,34	243,93	56°/55°	49,95	45,94

Based on the results of the calculation, the crack location schemes are constructed (Fig. 2). The angle of inclination of the main cracks according to fracture schemes 1 and 3 in all reinforcement variants is greater than 45°, therefore, the junction point of the inclined cracks at l 1/l 2 ≤ 2 is located on the plate field. According to the second fracture scheme and the results of the calculation of the reinforcement schemes under consideration, the angle of inclination of the cracks varies in the range of 41°÷43° (relative to the short side of the plate), therefore, the two main inclined cracks passing from the corners towards the non-supported side do not converge on the plate field.

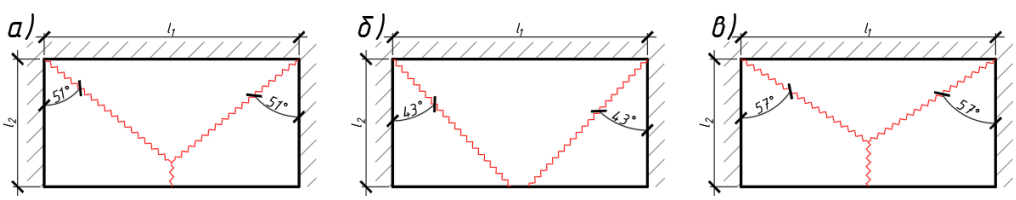

Fig. 2. Fracture schemes of plates according to the results of the calculation: a – according to Fig. 1,a; b – according to Fig. 1,b; c – according to Fig. 1, c.

When the dimensions of the support sections of the plates change by 3x1.5 m, the fracture schemes are preserved, the calculated angle of inclination of the cracks increases to 52°÷56° (relatively short side of the plate), which confirms the possibility of using the calculation method for plates with smaller dimensions (Table 4).

Table 4. Load-bearing capacity of slabs with dimensions of 3x1.5 m according to 1 destruction scheme.

Ø reinforcements	**Bending moments, kN·m**				**Calculated angle of crack inclination at variable and constant reinforcement pitch, φ**	**Maximum design loads at variable reinforcement pitch, kN/m2**	**Maximum design loads at a constant reinforcement pitch, kN/m2**	**Maximum design loads for reinforcement in one direction, kN/m2**
	M_1'	M_1''	M_1	M_2		$q_{\text{п}}^{\text{теор}}$	$q_{\text{п}}^{\text{теор}}$	$q_{\text{п}}^{\text{теор}}$
6	26,76	14,9	25,4	21,2	56°/53°	42,84	32,3	15,86
8	43,75	24,45	40,03	35,05	56°/53°	69,15	53,01	25,92
10	67,93	38,11	58,41	55,45	56°/52°	105,2	82,86	40,25

The load-bearing capacity of the plates is estimated according to the lowest of the values obtained, i.e. according to the calculated rupture loads determined according to the first scheme (Table 1). We will take as a basis the reinforcement of Ø10 class A400. Calculated rupture load at variable pitch $q_{\text{п}}^{\text{теор}} = 20{,}6\ \text{кН/м}^2$, at constant pitch $q_{\text{п}}^{\text{теор}} = 18{,}09\ \text{кН/м}^2$. The difference in rupture loads is 20.6 – 18.09 = 2.51 kN/ m2, which is approximately 12%. The obtained result confirms the fact that multilayer plates supported on three sides with a constant reinforcement pitch have insufficient strength in comparison with plates with variable-pitch reinforcement.

To increase the bearing capacity of plates with a constant reinforcement pitch to the level of the bearing capacity of plates with a variable pitch, it is necessary to increase the value of the bending moment M 1, which ultimately will lead to an increase in the reinforcement coefficients and additional consumption of reinforcing steel.

4 Conclusions

Based on the results of the study, the following conclusions can be drawn:

1. When changing the diameter of the reinforcement and the overall dimensions of the supported sides of multilayer floor slabs (supported on three sides, two short and one long), the fracture schemes remain unchanged and consist in the formation of two inclined cracks that converge on the plate field (1 and 3 schemes), as well as two inclined cracks that do not converge on the plate field (2 diagram).
2. It is recommended to calculate the load-bearing capacity of multilayer floor slabs supported on three sides (two short and one long) according to the 1st scheme based on the limit equilibrium method according to the formula (3).
3. According to the results of the calculation of multilayer floor slabs with different diameters of reinforcing rods, as well as when changing the main overall dimensions, it is recommended to perform reinforcement with a variable pitch of working reinforcement along the long side and with a constant pitch along the short side.

References

1. Tho Vu Dinh, E.A. Korol, V.I. Rimshin, Pham Tuan Anh Model of stress-strain state of three-layered reinforced concrete structure by the finite element methods International Journal for Computational Civil and Structural Engineering. 2022. Vol. 18(2) pp. 62-73.
2. V.D. Tho, E.A. Korol, N.I. Vatin, Duc H.M. The stress–strain state of three-layer precast flexural concrete enclosure structures with the contact interlayers Buildings 2021 Vol. 11(3) pp. 1-17.
3. E.A. Korol, V.D. Tho Bond strength between concrete layers of three-layer concrete structures IOP Conference Series: Materials Science and Engineering. International Conference on Civil, Architectural and Environmental Sciences and Technologies, CAEST 2019. 2020 pp. 012115.
4. D.T. Vu, E. Korol, Y. Kustikova, H.H. Nguyen Finite element analysis of three-layer concrete beam with composite reinforcement E3S Web of Conferences. 22nd International Scientific Conference on Construction the Formation of Living Environment, FORM 2019. 2019 pp. 02023.
5. E. Korol, Dinh Tho V., Huy Hoang N. Analysis the effects of lightweight concrete in the middle layer of multi-layered reinforced concrete structures on the stress-strain state using the finite element method MATEC Web of Conferences. 2018 pp. 02022.
6. E. Korol, Tho V.D., Y. Kustikova Model of stressed-strained state of multi-layered reinforced concrete structure with the use of composite reinforcement IOP Conference Series: Materials Science and Engineering. 21, Construction - The Formation of Living Environment. 2018. pp. 052033.
7. A.N. Neverov, E.S. Ketsko, P.S. Truntov, V.I. Rimshin Calculating the strengthening of construction structures before the reconstruction of the building Lecture Notes in Civil Engineering. 2022. Vol. 182. pp. 173-179.
8. V.I. Rimshin, V.I. Telichenko, P.S. Truntov, A.L. Krishan, G.S. Bykov Assessment of the impact of high temperature on the strength of reinforced concrete structures during operation Key Engineering Materials. 2021. Vol. 887 KEM. pp. 460-465.
9. V. Rimshin, P. Truntov Calculation and strengthening of reinforced concrete floor slab by composite materials Advances in Intelligent Systems and Computing. 2020. Vol. 1116. pp. 438-445.
10. M. Lukin, V. Martynov, V. Rimshin, I Aleksiievets. Reinforced concrete vertical structures under a gently sloping shell of double curvature under the influence of progressive collapse Lecture Notes in Civil Engineering. 2022. Vol. 182. pp. 577-587.
11. A.A. Varlamov, V.I. Rimshin, A. Davydov, A.R. Minnatov, A.M. Kurbatov Research of the degradation process of reinforced concrete structures IOP Conference Series: Materials Science and Engineering. 2021. Vol. 1079. pp. 062005.
12. E.S. Kuzina, V.I. Rimshin Calculation method analysis for structure strengthening with external reinforcement IOP Conference Series: Materials Science and Engineering. International Science and Technology Conference "FarEastCon 2019". 2020. pp. 022004.
13. A. L. Krishan, V. I. Rimshin, V. I. Telichenko, V. A. Rakhmanov, M. Y. Narkevich u 2017 Practical implementation of the calculation of the bearing capacity trumpet-concrete column Izvestiya Vysshikh Uchebnykh Zavedenii, Seriya Teknologiya Tekstil'noi Promyshlennosti 2017-January(2) 227–232.
14. S.A. Korotaev, V.I. Kalashnikov, V.I. Rimshin, I.V. Erofeeva, V.L. Kurbatov 2016 The impact of mineral Aggregates on the thermal conductivity of cement composites Ecology, Environment and Conservation 22(3) 1159–1164.
15. E. Kuzina, V. Rimshin, V. Kurbatov The Reliability of Building Structures Against Power and Environmental Degradation Effects 2018IOP Conference Series: Materials Science and Engineering 463(4) 042009.